3rd IAHR International Meeting of the Workgroup on Cavitation and Dynamic Problems in Hydraulic Machinery and Systems, October 14-16, 2009, Brno, Czech Republic

Hydrodynamic Damping Identification from an Impulse Response of a Vibrating Blade

Steven ROTH*

EPFL Laboratory for Hydraulic Machines, Switzerland

Martin CALMON

EPFL Laboratory for Hydraulic Machines, Switzerland

Mohamed FARHAT

EPFL Laboratory for Hydraulic Machines, Switzerland

Cécile MUENCH

EPFL Laboratory for Hydraulic Machines, Switzerland

Bjoern HUEBNER

Voith Hydro Holding GmbH & Co. KG, Germany

François AVELLAN

EPFL Laboratory for Hydraulic Machines, Switzerland

ABSTRACT

In the present study, the identification of hydrodynamic damping is investigated in the case of 2D blade placed in the test section of the EPFL High Speed Cavitation Tunnel. A non intrusive technique, based on a spark generated bubble, is used to generate a wide band mechanical excitation. An underwater electric discharge at the bottom of the test section creates a fast growing and collapsing bubble which generates strong shock waves in the test section. The response of the blade to this excitation impulse is monitored with the help of a digital Laser Doppler vibrometer. Assuming a Single Degree of Freedom (SDOF) system, the hydrodynamic damping is estimated in the time domain by fitting an exponentially damped function on the impulse response envelope. Tests are performed for flow velocities ranging from rest up to 15 m/s. A linear relationship is found between the hydrodynamic damping and the reduced flow velocity for the first bending mode, while surprisingly a constant damping factor is experienced for the first torsion mode.

KEYWORDS

Hydrodynamic damping, vibrations, impulse response, non-intrusive mechanical excitation.

* *Corresponding author: EPFL Laboratory for Hydraulic Machines, Av. de Cour 33 bis, CH-1007 Lausanne, Switzerland, phone: +41 (0)21 693 25 63, email: steven.roth@epfl.ch*

1. INTRODUCTION

The hydrodynamic damping is the fluid contribution to the total damping, also including structural and material damping, of an immersed vibrating structure. This damping is one of the main parameters that influence the amplitude of vibrations. It is directly related to fatigue problems in hydraulic machines which are of great importance in their design procedure. Thus, the identification of hydrodynamic damping is crucial for constructors who, nowadays, try more and more to assess the dynamics of runners at the earliest stage of the design phase.

Several works on hydrodynamic damping are related to pipes, struts and cables (Blevins [1]) or to cylinder (Chaplin, [2]), but very few directly to blades (Kaminer [3]). The latter verified experimentally the linear behavior of the hydrodynamic damping against a reduced flow velocity. This dependence shows good agreement with potential flow theory and the linearization of fluid forces (Theodorsen [4]).

The identification of a blade hydrodynamic damping is influenced by many different parameters, such as the flow velocity, the fluid density (Kaminer [3]) and the flow velocity field around the blade. Moreover, the fluid environment makes the excitation of an immersed structure difficult. The aim of this paper is to identify the hydrodynamic damping in a reliable way and to determine the influence of the flow velocity. The damping could be directly identified from the flow-induced vibrations, but, the turbulent noise level being too high, the impulse response, which enables a much better damping identification, is chosen. The present paper suggests thereby a non-intrusive impulse excitation procedure.

In this paper, the experimental setup, as well as the test case, is first described. The physical model is then exposed. Finally, the results on hydrodynamic damping both in still water and in flow with different flow velocities are given.

2. EXPERIMENTAL SETUP

The experimental investigations are conducted in the EPFL High Speed Cavitation Tunnel (Avellan et al. [6]), presented in Fig. 1. Blades are installed in the 0.150 x 0.150 x 0.750 m test section, enabling all possible flow incidence angles; a maximum inlet velocity of 50 m/s being reached. The test section static pressure is controlled, up to 1.6 MPa for controlling both the onset and the development of cavitation.

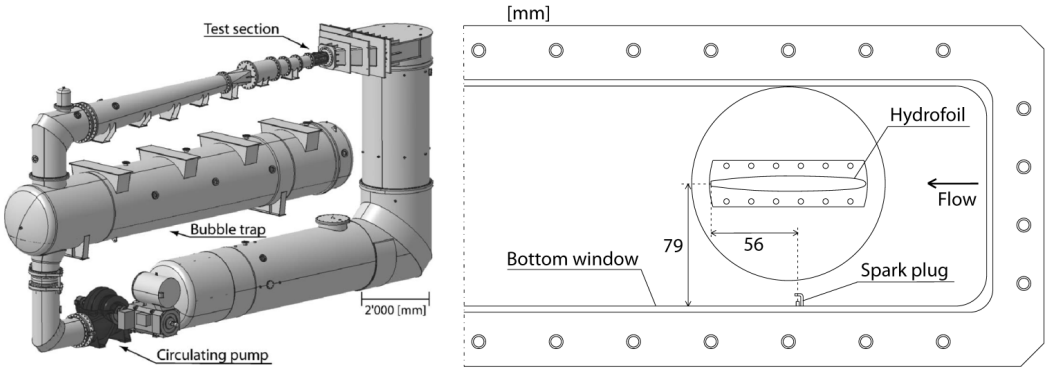

Fig. 1: EPFL High Speed Cavitation Tunnel (left) and details of the blade and spark plug installation in the test section (right)

An original system is used to create an impulse excitation. A spark plug (Pereira et al. [7]) is mounted in the bottom window of the test section (Fig. 1) 56 mm away from the blade trailing edge in the test section mid-span. When the spark is generated with the discharge of 1'550 nF capacitor, a rapid increase of the water temperature is produced. A vapor bubble grows in an

explosive way generating strong shock waves travelling towards the blade and providing an impulse excitation. The bubble then collapses and rebounds several times. Nevertheless, the relevant exciting pressure impulse is related to the first shock wave created. The time history of an expanding and collapsing bubble, visualized with a high speed PHOTRON FASTCAM SA1.1 camera[1], for 5 m/s flow velocity and 0.1 MPa static pressure, is given in Fig. 2. Within the flow velocity range investigated, the bubble remains close to its original location. The shock waves generated by the bubble expansion travel with the speed of sound in water, i.e. 1'485 m/s, inducing a pressure excitation of very short duration and therefore addressing a wideband frequency range.

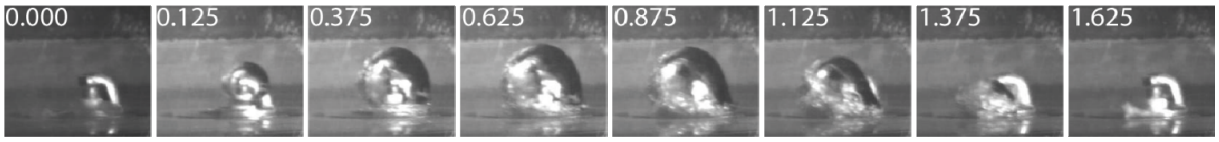

Fig. 2: Time history of the spark generated bubble (time in ms), 5 m/s flow velocity, 0.1 MPa Static pressure, 6.5 mm maximum radius

The structural vibration velocity is measured with a Laser Doppler Vibrometer, Polytec PDV-100[2]. Vibration signals are digitized at 51.2 kHz sampling frequency over 0.32 seconds yielding a 3.125 Hz frequency resolution.

3. TEST CASE

A 2D symmetric modified NACA0009 blade, see Fig. 3, made of stainless steel featuring E =215 GPa Young modulus, ρ_s = 7700 kg/m^3 density and ν = 0.3 Poisson's ratio is investigated. The cantilever blade is clamped at one end, the 150 mm blade span, from the free tip, being subjected to the flow.

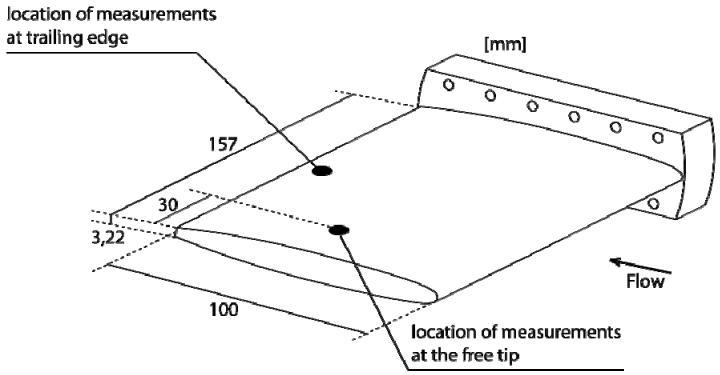

Fig. 3: 2D NACA0009 blade and locations of the vibration velocity measurement points

The two first eigen modes of the blade are of interest in the present study: the 1st bending mode (mode 1) and the 1st torsion mode (mode 2) shown in Fig. 4.

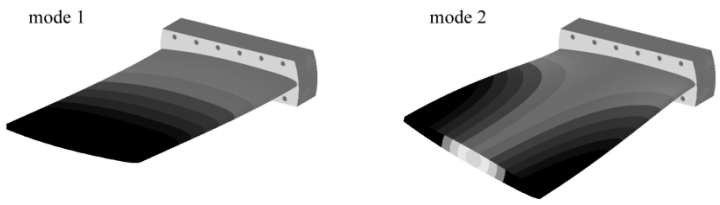

Fig. 4: First two eigen modes: bending (left) and torsion (right)

[1] http://www.photron.com/pdf/Fastcam_SA1_Datasheet.pdf
[2] http://www.polytec.com/int/_files/LM_BR_PDV-100_2007_03_E.pdf

The flow velocity is set from 2 m/s to 17 m/s, and the incidence angle is kept at 0°. The pressure level is adjusted as the flow velocity is increased to prevent cavitation onset.

4. PHYSICAL MODEL

As illustrated on Figure 5, the case study may be simplified into a Single Degree of Freedom (SDOF) linear system. The only variables are the structure displacement y , the velocity $\dot{y}$ and the acceleration $\ddot{y}$.

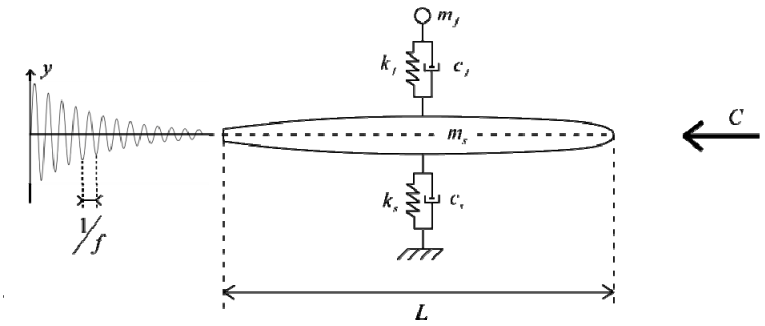

Fig. 5: Simplified model of a vibrating immersed blade

Following the classical analytical approach, the vibrating system is governed by Eq.(1), where the mass, stiffness and damping of the structure are respectively denoted by m_s, k_s and c_s, and the mass, stiffness and damping added by the surrounding fluid are denoted by m_f, k_f and c_f. The flow-induced excitation force is denoted by $F(t)$.

$$\left(m_s + m_f\right)\ddot{y} + \left(c_s + c_f\right)\dot{y} + \left(k_s + k_f\right)y = F(t) \tag{1}$$

Divided by the vibrating system total mass, Eq.(1) can be written:

$$\ddot{y} + 2\zeta\omega_n\dot{y} + \omega_n{}^2 y = \tilde{F} \tag{2}$$

with ζ being the total damping factor, or total damping coefficient, and ω_n, the eigen pulsation. The reduced flow velocity C^* is defined as the ratio between one period of the structural vibrations and the time that a fluid particle takes to travel from the leading edge to the trailing one.

$$C^* = \frac{C}{f \cdot L} \tag{3}$$

where C is the flow velocity, L is the profile chord length and f is the blade oscillations frequency.

5. RESULTS

The total damping of an immersed blade consists of the sum of structural, material and hydrodynamic damping. The two first terms are not identified in the present study, but are generally assumed to be much lower than the hydrodynamic damping. Therefore, no distinction is made in the present paper between total damping and hydrodynamic damping.

The flow induced vibrations are caused by the turbulence in the boundary layer and mainly by vortex shedding in the wake (Blevins, [1]). Therefore, the damping could be determined directly from the flow-induced excitation. However, a much better excitation of both eigen modes can be observed, and a greater level of response is obtained when using the non-intrusive spark generated bubble excitation than when letting the flow alone excite the blade, as it can be observed by comparing Fig. 6 with Fig. 7.

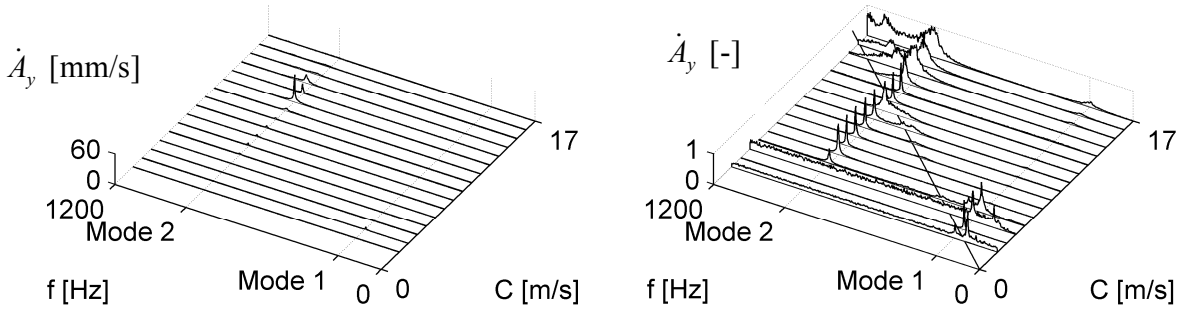

Fig. 6: Laser vibrometer signals amplitude spectra (measurements at trailing edge) without spark generated bubble excitation for different flow velocities (left), normalized (right) and linear vortex shedding frequency law

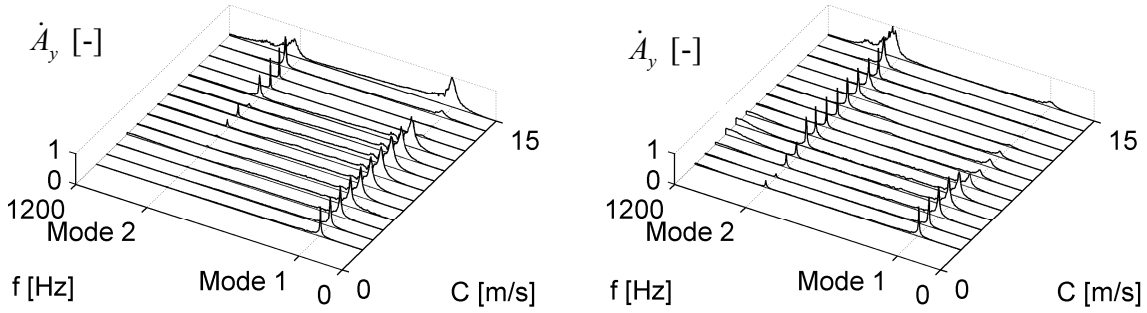

Fig. 7: Normalized Laser vibrometer signals amplitude spectra for different flow velocities, for tip centered (left) and trailing edge (right) measurement points

The lock-in phenomenon has been largely investigated at EPFL by Ausoni, [5]. This phenomenon is visible in Fig. 6 (right), where each spectrum has been normalized by its maximum. Lock-in occurs, as expected, for the flow velocity values close to 3 m/s and between 12 m/s and 13 m/s, respectively for the first and second eigen modes of the blade.

In lock-off conditions, neglecting the turbulence noise, the free decay method can be used for the damping identification (Blevins [1]). If the blade is subjected to an excitation of amplitude A_y and then the excitation is released, the vibrations decrease slowly in time. $\tilde{F}$ is set to zero in Eq.(2) and the resulting structural displacement is given by the Eq.(4) for $t > 0$:

$$y = A_y e^{-\zeta\omega_n t} \sin\left(\omega_n \sqrt{1-\zeta^2}\, t + \phi\right) \tag{4}$$

For a lightly damped system, $\zeta < 1$, looking at the ratio of amplitude between N successive peaks leads to the logarithmic decrement equation:

$$2\pi\zeta N = \log\left(\frac{A_i}{A_{i+N}}\right) \tag{5}$$

In this study, the time signal is first filtered to take into account the onset of several eigen modes. A Butterworth low-pass filter is applied on the original signal to isolate the first mode whereas a Butterworth band-pass filter centered on the second eigen frequency is used to cope with the second mode. The characteristics of the filters are given in Tab. 1.

	Cut-off frequency [Hz]		Filter order [-]	
	mode 1	**mode 2**	**mode 1**	**mode 2**
Filter type	Low-pass	Band-pass	Low-pass	Band-pass
Stainless Steel	400	[750 1050]	6	4

Tab. 1: Butterworth filters properties

Then, by applying a Hilbert transform, the envelope of this filtered signal is obtained. Finally, an exponential fitting is applied for computing the damping factor. The total damping value is averaged over ten records. Fig. 7 shows the averaged spectra from these ten records, for the two measurement points shown in the Fig. 3. Indeed, the tip centered point is chosen when focusing on the bending mode, whereas the trailing edge point is used for the torsion mode. In this way, a kind of mechanical filtering is applied. Fig. 8 shows how the filtered signal differs from the original signal and shows the shape of the envelope (time axis is reduced for better insight) for the case of still water.

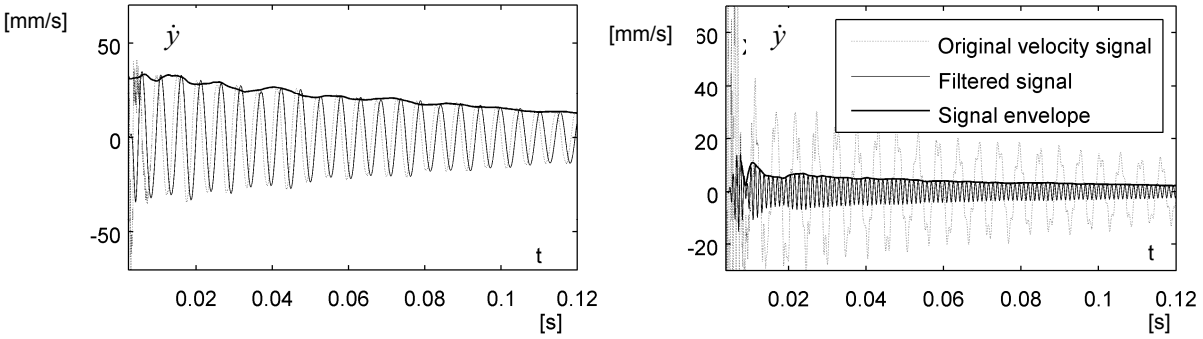

Fig. 8: Damping identification from the time Laser vibrometer signals in still water for the bending mode (left) and the torsion mode (right)

The hydrodynamic damping is plotted versus the reduced flow velocity in Fig. 9. For the first eigen mode, the 3 m/s, 12 m/s and 13 m/s flow velocities are excluded because of lock-in conditions. For the second eigen mode, the flow velocities above 5 m/s are excluded since the flow permanently excites the blade and the hypothesis of free decay is no longer valid. The flow velocities above 15 m/s are excluded for both eigen modes due to a dominant turbulent noise.

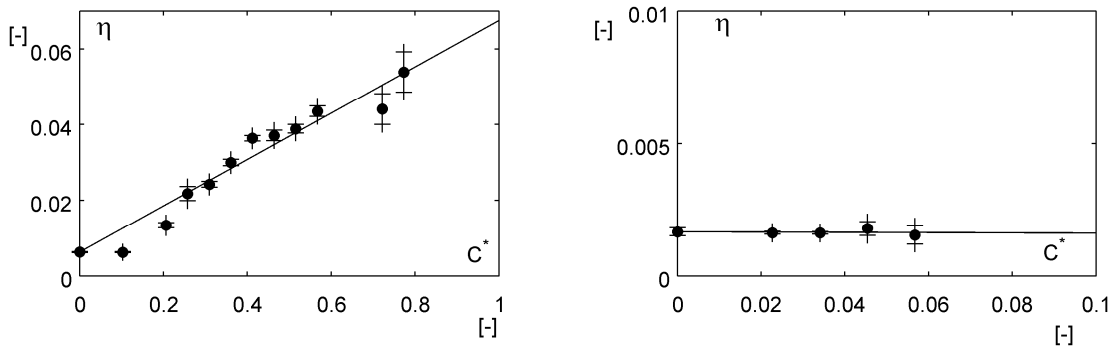

Fig. 9: Total damping against reduced flow velocity for the 1st bending mode (left) and the 1st torsion mode (right), with both flow and spark bubble explosion excitations

Results are summarized in Tab. 2. A linear dependence of the hydrodynamic damping with the reduced flow velocity is found for the first eigen mode, whereas a constant damping is obtained for the second eigen mode. The corresponding reduced flow velocity range is nevertheless not the same. The hydrodynamic damping coefficient of the torsion mode in still

water is approximately four times lower than the one of the bending mode mainly due to frequency ratio between the two eigen modes.

	Frequency [Hz]	Damping in still flow [-]	Damping slope [-/-]
mode 1	194	$6.3 \cdot 10^{-3}$	$61.2 \cdot 10^{-3}$
mode 2	880	$1.7 \cdot 10^{-3}$	$-0.5 \cdot 10^{-3}$

Tab. 2: Hydrodynamic damping for the two eigen modes

6. CONCLUSION

In the present study, we have carried out experimental investigations on a 2D cantilever NACA0009 blade placed in the EPFL High Speed Cavitation Tunnel, to address the issue of hydrodynamic damping identification. A specific non-intrusive procedure, based on a spark generated bubble which induces a shock wave, is successfully used to excite the blade on a wide frequency range. The displacement velocity of structural vibrations is measured with the help of a Laser Doppler vibrometer. The hydrodynamic damping of the first eigen mode is found to depend linearly with the reduced flow velocity, whereas the one relative to the second eigen mode remains constant. The proposed procedure for hydrodynamic damping identification is found appropriate as far as the flow induced vibrations does not perturb the blade response to the spark generated bubble.

7. ACKNOWLEDGEMENTS

The present investigation was carried out in the frame of HYDRODYNA project (Eureka N° 3246), in a partnership with ALSTOM Hydro, ANDRITZ Hydro, VOITH Hydro and UPC-CDIF. The authors would like to thank the Swiss Federal Commission for the Technology and Innovation (CTI) and Swisselectric Research for their financial support as well the HYDRODYNA partners for their involvement and support.

8. REFERENCES

[1] Blevins, R. D.: *Flow-induced vibrations*, Van Norstrand Reinhold. New York. 1990.

[2] Chaplin, J.R., and K. Subbiah. Hydrodynamic damping of a cylinder in still water and in a transverse current. *Applied Ocean Research*, 1998. 251-259.

[3] Kaminer, A.A., and N. Ya. Nastenko. : Experimental investigation of hydrodynamic damping during bending oscillations of blade profiles in water flow. *Strength of Materials*, 1976: 25-27.

[4] Theodorsen, Th., General Theory of Aerodynamic Instability and the Mechanism of Flutter. NACA Report 496. 1935.

[5] Ausoni, Ph., Farhat M., Escaler X., Egusquiza E. and Avellan F.: Cavitation Influence on von Kármán Vortex Shedding and Induced Hydrofoil Vibrations, *Journal of Fluid Engineering*, 2007.

[6] Avellan F., Henry P., and Ryhming I.L.: A New High Speed Cavitation Tunnel, *ASME Winter Annual Meeting*, Boston, MA, Vol. 57, pp. 49-60, 1987.

[7] Pereira F., Farhat M., Avellan F.: Dynamic calibration of transient sensors by spark generated cavity. *Proceeding of IUTAM Symposium on Bubble Dynamics and Interface Phenomena*, 1993.

9. NOMENCLATURE

$A_v, \dot{A}_v$	[m]	initial amplitude of the structural displacement, velocity
C	[m/s]	flow velocity
C^*	[-]	reduced flow velocity
E	[GPa]	material Young modulus
$F, \tilde{F}$	[N]	flow-induced excitation force, acceleration
L	[m]	chord length of the blade
c_s	[kg/s]	structure damping matrix
c_f	[kg/s]	fluid damping matrix
f	[Hz]	blade oscillations frequency
k_s	[Pa]	structure stiffness matrix
k_f	[Pa]	fluid stiffness matrix
m_s	[kg]	structure mass matrix
m_f	[kg]	added mass matrix
t	[s]	time
$y, \dot{y}, \ddot{y}$	[m]	structural displacement, velocity and acceleration
ϕ	[rad]	phase of the free decay displacement response
ν	[-]	material Poisson's coefficient
ρ_s	[kg/m^3]	material Density
ω_n	[rad/s]	eigen pulsation of a structure in water
ζ	[-]	total damping factor